A Design Method of A Robust Controller for Hydraulic Actuation with Disturbance Observers

Hiroaki Kuwahara, Fujio Terai
Corporate Manufacturing Engineering Center,
TOSHIBA Corporation,
Yokohama, Japan
Email: hiroaki.kuwahara@toshiba.co.jp,
fujio.terai@toshiba.co.jp

Michele Focchi, Gustavo A. Medrano–Cerda,
Darwin G. Caldwell, and Claudio Semini
Department of Advanced Robotics,
Istituto Italiano di Tecnologia (IIT),
Genoa, Italy
Email: Michele.Focchi@iit.it, Gustavo.Cerda@iit.it,
Darwin.Caldwell@iit.it, Claudio.Semini@iit.it

***Abstract*—In this paper, a design method of a robust controller for hydraulic actuators is proposed. Generally speaking, the hydraulic actuator generates hydraulic force, and a load is driven by the hydraulic force. In order to control the hydraulic actuators, non-linearity caused by chamber pressures and natural feedback meaning the effect by the load velocity on the hydraulic pressure dynamics should be considered. A controller with feedback linearization is one of the methods to compensate the effects of the non-linearity and the natural feedback. However, since the method is based on the model parameters of the hydraulic actuator, the control performance is affected by modeling errors and modeling uncertainties. Therefore, a robust controller for the hydraulic actuator is proposed to complement the disadvantage of the conventional method. To design the proposed controller, a part of the feedback linearization, that is, pressure (non-linearity) compensation is used to linearize the hydraulic pressure dynamics virtually. By using the virtually linearized hydraulic dynamics and the nominal mass, the nominal model of the hydraulic pressure and that of the load motion dynamics model are designed. Then, the effects which prevent each dynamics from behaving as the nominal models are defined as disturbances. In the proposed controller, two types of the observers are designed to compensate the disturbances. In this paper, the design details are shown and the validity of the proposed method is shown by simulation and experiments.**

I. Introduction

In industrial fields, automation of the manual process has been carried out to improve production efficiency and decrease production costs. Especially, it is required to replace man power with robots for manipulation task of heavy materials, since this task needs a lot of human strength.

In order for the robots to handle the heavy materials, a hydraulic actuation system has been used due to its high-power density and large force/torque output. In general, a hydraulic actuator is composed of a hydraulic system and a mechanical system. A basic hydraulic system consists of a valve, a cylinder, and a pump, and it generates hydraulic pressure dynamics. The hydraulic pressure is converted to the force/torque and transmitted to the mechanical system. The mechanical system such as a load is linked rigidly to the hydraulic system and drives. Here, the hydraulic force dynamics has non-linearity caused by cylinder chamber pressures. In addition, the velocity from the mechanical system deteriorates the pressure tracking (afterwards, this effect is called "natural feedback") [1]. Therefore, the non-linearity and the natural feedback should be considered when the hydraulic actuator is controlled [2].

As counter measures to the non-linearity, some design methods for the hydraulic actuator have been proposed with passivity-based control [3] [4], sliding mode control [5], back-stepping method [6], and with feedback linearization [7] [8]. In previous work [9] [10], the authors focused on the method with the feedback linearization since the feedback linearization compensates not only the effects of the non-linearity, but also that of the natural feedback. Since this method is based on the physical model, the controller can be designed based on the physical parameters. But, on the other hand, modeling errors and model uncertainty directly affect system performance. In the hydraulic actuator, such model errors and model uncertainty are unavoidable. This is because some parameters like the oil bulk modulus changes with its temperature and is thus difficult to identify [11]. Therefore, in this method, it is necessary to tune the gains those scale the level of the compensation.

In this paper, a robust controller is proposed to complement the disadvantage of the feedback linearization method. To design the proposed controller, a part of the feedback linearization, that is, pressure (non-linearity) compensation is used to linearize the hydraulic pressure dynamics virtually. By using the virtually linearized hydraulic dynamics and the nominal mass, the nominal model of the hydraulic pressure and that of the load motion dynamics are designed. Then, the effects which prevent each dynamics from behaving as the nominal models are defined as disturbances. The proposed controller is composed of two kinds of disturbance observers [12], and compensates the disturbances. This controller functions to improve the robustness against the modeling error and the model uncertainty while the effects of the non-linearity and the natural feedback are alleviated.

This paper is organized as follows: the structure of the target hydraulic system is described in Section II. The proposed robust controller for the hydraulic actuator is presented in Section III. The validity of the proposed method is confirmed by simulation and experiment in Section IV. Conclusions are described in Section V.

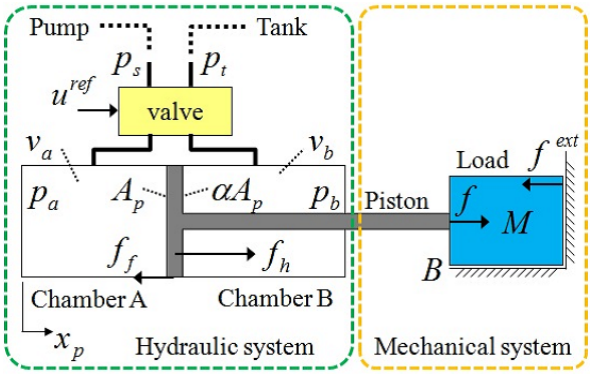

Fig. 1. Target hydraulic actuation system.

II. Hydraulic system dynamics

A. System description

Fig. 1 shows the hydraulic actuator treated in this paper. As shown in Fig. 1, the hydraulic actuator consists of the hydraulic system and the mechanical system. In the hydraulic system, the fluid circulates between a pump and a tank. Here, the supply pressure of the fluid is defined as p_s, and the tank pressure is defined as p_t. And, according to the control reference u^{ref}, the valve controls direction and magnitude of the flows to the asymmetric cylinder. These flows change the chamber pressures p_a and p_b and the volumes of the chambers v_a and v_b. The chamber pressures generate the hydraulic force f_h as follows

$$f_h = A_p p_a - \alpha A_p p_b = A_p(p_a - \alpha p_b). \tag{1}$$

where A_p is a piston area, and αA_p is the annular area which is defined by a factor of α $(0 < \alpha < 1)$. Consequently, the force f is transmitted to the mechanical system, which takes into account the cylinder friction force f_f. The mechanical system is simplified in this schematic to be an inertial load with constant mass M and friction B. f^{ext} denotes the external force to the load except the friction force. Since the hydraulic system and the mechanical system are linked rigidly, the piston position x_p in the hydraulic system can be obtained by measuring that of the mechanical system. When the mechanical system is driven by the hydraulic force, the velocity $\dot{x}_p$ goes back to the hydraulic system, this is called natural feedback.

B. Load pressure dynamics

In this paper, a load pressure p_l is defined using the cylinder chamber pressures p_a and p_b as (2). It is the pressure that effectively produces the force.

$$p_l \triangleq \frac{f_h}{A_p} = p_a - \alpha p_b \tag{2}$$

If the valve dynamics is ignored, the load pressure dynamics is represented as

$$\begin{aligned} \dot{p}_l &= \beta_e(Gu^{ref} + F\dot{x}_p) \qquad (3)\\ G &= K_v \left\{ \frac{\sqrt{(\frac{p_s - p_t}{2}) + sign(u^{ref})(\frac{p_s + p_t}{2} - p_a)}}{v_a} \right.\\ &\quad \left. + \alpha \frac{\sqrt{(\frac{p_s - p_t}{2}) + sign(u^{ref})(p_b - \frac{p_s + p_t}{2})}}{v_b} \right\}\\ F &= -A_p \left\{ \frac{1}{v_a} + \frac{\alpha^2}{v_b} \right\} \end{aligned}$$

where β_e and K_v denote the bulk modulus and valve gain, respectively. From (3), the load pressure dynamics is controlled by the control reference u^{ref}, but is affected by the velocity $\dot{x}_p$. F and G change dynamically based on the cylinder chamber pressures and volumes. Especially, G is non-linear with changing the chamber pressures. Therefore, it can be said that the non-linearity and the natural feedback should be considered to control the hydraulic actuator.

C. Feedback linearization

The control method with the feedback linearization is a candidate to alleviate the effects of the non-linearity and the natural feedback. In this method, the reference to the actuator u_a^{ref} is computed using the estimated functions $\hat{F}$ and $\hat{G}$ as follows

$$u_a^{ref} = \frac{1}{\hat{G}}(u^{ref} - \hat{F}\dot{x}_p). \tag{4}$$

In (4), the subtraction of $\hat{F}\dot{x}_p$ from the control reference u^{ref} is called velocity compensation, and the division of the result by the estimated $\hat{G}$ is called pressure (non-linearity) compensation. If the estimation of $\hat{F}$ and $\hat{G}$ is perfect, that is $\hat{F} = F$ and $\hat{G} = G$, the load pressure p_l can be controlled by the control reference u^{ref} without the natural feedback as follows

$$\dot{p}_l = \beta_e u^{ref}. \tag{5}$$

Since this method is based on the physical model, it can improve the system development efficiency. But, on the other hand, the real systems suffer from the model uncertainty errors, which affect the system performance. Therefore, from the practical viewpoint, it is necessary to adjust the level of compensation by using a pressure compensation gain k_{pc} and a velocity compensation gain k_{vc} as follows

$$u_a^{ref} = \frac{k_{pc}}{\hat{G}}(u^{ref} - k_{vc}\hat{F}\dot{x}_p). \tag{6}$$

Since the k_{pc} and k_{vc} do not have any physical meaning, it is difficult to tune the gains correctly.

III. Design of the proposed controller

In this section, the disturbances to the hydraulic actuator including the effects by the modeling error and the modeling uncertainty are defined. Then, the robust controller is designed to compensate the disturbances.

A. Load pressure dynamics and load motion dynamics including the modeling error and the modeling uncertainty

When the effect of pressure drop by oil leakage is considered, the load pressure dynamics as shown in (3) can be rewritten as follows

$$\dot{p}_l = \beta_e(Gu^{ref} + F\dot{x}_p) - C_l(p_a, p_b) \tag{7}$$

where$C_l(p_a, p_b)$ denotes the function to show the pressure drop by oil leakage. In addition, by introducing nominal values and modeling error, β_e, G and F in (7) can be expressed as follows

$$\beta_e = \beta_{en} + \Delta\beta_e \tag{8}$$
$$G = G_n + \Delta G \tag{9}$$
$$F = F_n + \Delta F \tag{10}$$

where subscript $_n$ means the nominal value and Δ means the modeling error. Here, ΔG in (9) includes the model errors of the valve gain K_v, the cylinder chamber volumes v_a and v_b, and the effects of the valve dynamics. ΔF in (10) includes the model errors of the cylinder chamber volumes v_a and v_b. From (7)$\sim$(10), the load pressure dynamics including the modeling error and the modeling uncertainty as follows

$$\dot{p}_l = \beta_{en}G_n u^{ref} + (\beta_{en}\Delta G + \Delta\beta_e G_n + \Delta\beta_e\Delta G)u^{ref} + (\beta_{en} + \Delta\beta_e)F\dot{x}_p - C_l(p_a, p_b). \tag{11}$$

On the other hand, the load motion dynamics is represented as follows

$$\begin{aligned} M\ddot{x}_p &= f - f^{ext} - B\dot{x}_p \\ &= A_p p_l - f_f - f^{ext} - B\dot{x}_p \end{aligned} \tag{12}$$

In the same way, by introducing nominal values and modeling error, M and A_p in (12) can be expressed as follows

$$M = M_n + \Delta M \tag{13}$$
$$A_p = A_{pn} + \Delta A_p \tag{14}$$

From (12)$\sim$(14), the load motion dynamics including the modeling error and the modeling uncertainty as follows

$$M_n\ddot{x}_p = A_{pn}p_l + \Delta A_p p_l - \Delta M\ddot{x}_p - f^{ext} - f_f - B\dot{x}_p. \tag{15}$$

B. Definition of the disturbance in hydraulic actuation

The disturbances to the hydraulic actuator can be classified into the disturbance to the hydraulic system q_h^{dis} and that to the mechanical system q_m^{dis} as shown in Fig. 2. Here, the pressure compensation is utilized to alleviate the non-linearity while the natural feedback can be included in the disturbance

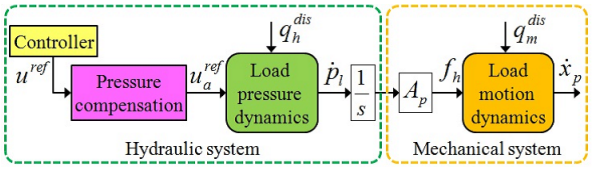

Fig. 2. Disturbances to the hydraulic actuation system. The disturbance to the hydraulic system q_h^{dis} affects the load pressure p_l. The disturbance to the mechanical system q_m^{dis} affects the load velocity $\dot{x}_p$.

to the hydraulic actuator. When the pressure compensation is utilized, the load pressure dynamics is represented as follows

$$\dot{p}_l = \frac{\beta_{en}G_n}{\hat{G}}u^{ref} + \frac{(\beta_{en}\Delta G + \Delta\beta_e G_n + \Delta\beta_e\Delta G)}{\hat{G}}u^{ref} + (\beta_{en} + \Delta\beta_e)F\dot{x}_p - C_l(p_a, p_b) \tag{16}$$

Since the ideal load pressure dynamics with the pressure compensation is defined as (17), the disturbance to the hydraulic system q_h^{dis} can be defined as (18).

$$\dot{p}_l = \frac{\beta_{en}G_n}{\hat{G}}u^{ref}, \tag{17}$$

$$q_h^{dis} = \frac{(\beta_{en}\Delta G + \Delta\beta_e G_n + \Delta\beta_e\Delta G)}{\hat{G}}u^{ref} + (\beta_{en} + \Delta\beta_e)F\dot{x}_p - C_l(p_a, p_b). \tag{18}$$

From (18), the disturbance to the hydraulic system includes the following things:

- the disturbance caused by the model uncertainty such as the internal oil leakage and the valve dynamics
- the disturbance caused by the modeling error of the pressure compensation and the load pressure dynamics
- the disturbance from the natural feedback.

On the other hand, since the ideal load motion dynamics is defined as (19), the disturbance to the mechanical system q_m^{dis} can be defined as (20).

$$M_n\ddot{x}_p = A_{pn}p_l \tag{19}$$

$$q_m^{dis} = \Delta A_p p_l - \Delta M\ddot{x}_p - f^{ext} - f_f - B\dot{x}_p \tag{20}$$

From (20), the disturbance to the mechanical system includes the following things:

- the external disturbance to the load such as the external force f^{ext} and the load friction $B\dot{x}_p$
- the cylinder friction force f_f
- the disturbance caused by the modeling error of the piston area A_p and the load mass M.

In order to estimate and compensate the disturbances, two types of disturbance observers [12] are designed. In this paper, one is defined as $DOB1$ for the disturbance to the hydraulic system, and the other is defined as $DOB2$ for the disturbance to the mechanical system. The disturbance observer estimates the disturbance using the difference between ideal and actual output. The ideal output can be calculated by the input and

nominal model parameters. The design of the $DOB2$ requires the nominal parameter of the piston area A_p and the load mass M. Basically, A_p can be obtained from the mechanical data sheet. M can be also obtained from the weight of the load with regard to the one-direction actuator as shown in Fig. 1, and calculated from the equivalent mass matrix defined as a function of Jacobian matrix and inertia of manipulator with regard to the multidegrees-of-freedom robot. However, to design the $DOB1$, it is necessary to identify the nominal load pressure dynamics model with the pressure compensation.

C. Modeling of the nominal load pressure dynamics

Since the right hand in (17) denotes the linearized load pressure dynamics by the control reference, the nominal load pressure dynamics model can be obtained from the relation between the control reference u^{ref} and the load pressure p_l with the pressure compensation. In this paper, the nominal load pressure model W_n was identified as a black-box model by applying the Random Gaussian Signal under the condition that the load velocity is zero. Though the nominal load pressure model W_n should be an integrator ideally, it was approximated as the first order lag model as follows

$$W_n = \frac{K_1}{1+T_1 s}. \tag{21}$$

There are two reasons why the first order lag model was selected. One reason is that the bandwidth of the model can be managed by using the gain K_1 and the time constant T_1 of the first order lag system. The other is that the lower order should be better, since the inverse nominal load pressure model W_n^{-1} is used in the design. In other words, the number of differentiation should be as low as possible in practical usage.

D. Design of the $DOB1$ and the $DOB2$

Fig. 3 shows the proposed robust controller for the hydraulic actuator. The $DOB1$ and the $DOB2$ have low-pass filters V_1

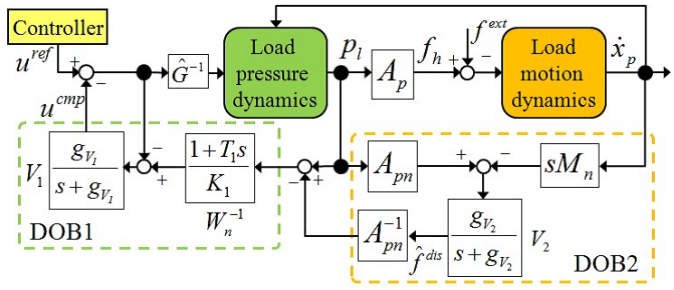

Fig. 3. Proposed robust controller for the hydraulic actuation system. The $DOB1$ compensates the disturbance to the hydraulic system with the identified inverse hydraulic dynamics W_n^{-1}. The $DOB2$ compensates the disturbance to the mechanical system with the nominal piston area A_{pn} and mass M_n.

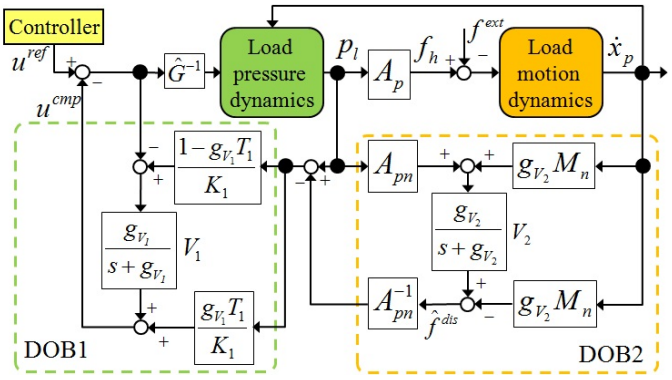

Fig. 4. The equivalent block diagram of the proposed robust controller in Fig. 3. This controller avoids differentiating the load pressure p_l in the $DOB1$ and the load velocity $\dot{x}_p$ in the $DOB2$.

and V_2, respectively. Each low-pass filter has cutoff frequencies g_{V_1} and g_{V_2} as shown in (22) and (23), respectively

$$V_1(s) = \frac{g_{V_1}}{s+g_{V_1}}, \tag{22}$$

$$V_2(s) = \frac{g_{V_2}}{s+g_{V_2}}. \tag{23}$$

The variables $\hat{f}^{dis}$ and u^{cmp} in the figure mean estimated disturbance force to the load, and compensation signal, respectively. As shown in Fig. 3, the estimated disturbance force $\hat{f}^{dis}$ by the $DOB2$ is transformed to the equivalent pressure by using A_{pn}^{-1}. The measured load pressure p_l and the equivalent pressure are combined, and the sum of the pressure information is one of the inputs to the $DOB1$. Then, the compensation signal u^{cmp} is computed by the $DOB1$. However, it is necessary to differentiate the load pressure p_l in the $DOB1$ and the load velocity $\dot{x}_p$ in the $DOB2$ and, in practice, differential calculation makes noise signals. Therefore, the block diagram as shown in Fig. 3 is transformed into the equivalent one as shown in Fig. 4 in order to avoid the differentiations.

The $DOB1$ is supposed to improve the hydraulic control performance, in other words, the $DOB1$ is expected to improve the outer force or position control performance. Also, the $DOB2$ is supposed to improve the robustness especially against load variations.

E. Force control with the proposed robust controller

In this paper, the proposed robust controller is applied to a force controller. The force controller computes the control reference u^{ref} to the proposed controller in order for the hydraulic force response f^{res} to track the force command f^{cmd}.

IV. Simulation and Experiments

In this section, the simulation and experimental results are shown to confirm the validity of the proposed method. At first,

TABLE I
SIMULATION CASES

$Case\ No.$	A_{pn}/A_p
$case\ 1$	1.0
$case\ 2$	0.9
$case\ 3$	0.5

TABLE II
NOMINAL PARAMETERS FOR THE $DOB1$ AND THE $DOB2$ IN SIMULATION

$DOB1$	K_1	2.5	$[MPa/mA]$
	T_1	2.0×10^{-3}	$[s]$
$DOB2$	A_{pn}	2.0×10^{-4}	$[m^2]$
	M_n	3.0	$[kg]$

simulations were done to show the robustness of the proposed method against modeling errors. Then, the experimental results are shown to demonstrate the effect of the proposed method for the force control performance.

A. Simulation

In the simulation, the robustness against the modeling error of the feedback linearization method and the proposed method are compared.

1) Simulation conditions: Since the parameter of the piston area A_{pn} is commonly used in both of the methods, the cases without/with the modeling error of the piston area are simulated. The conditions of the modeling error for the simulation are shown in Table I. In both methods, the force controller is used for the force response f^{res} to track the force step command $f^{cmd} = 500[N]$. A proportional gain K_p is used in the force controller, and the gain was tuned to converge a step response smoothly for each method. The gain was set to $K_p = 5.0 \times 10^{-4}$ for the conventional method, and $K_p = 1.0 \times 10^{-6}$ for the proposed method. In the conventional method, the pressure compensation gain k_{pc} and the velocity compensation gain k_{vc} were set as 1. The cutoff frequencies for the $DOB1$ and the $DOB2$ are set to $50[rad/s]$. The nominal model parameters for the $DOB1$ and the $DOB2$ are shown in Table II.

2) Simulation results: Fig. 5 and Fig. 6 show the simulation results with the conventional method and the proposed method, respectively. In Fig. 5, the force response f^{res} with the conventional method was deteriorated by increasing the modeling error. This result shows that the conventional method can be easily affected by the modeling error. On the other hand, from Fig. 6, few changes in the force response can be observed when the modeling error increases. From these results, the robustness against the modeling error was improved by the proposed method.

Though only one modeling error was simulated in this paper, the same results can be obtained by changing the other modeling errors. Especially, in the field of the hydraulic

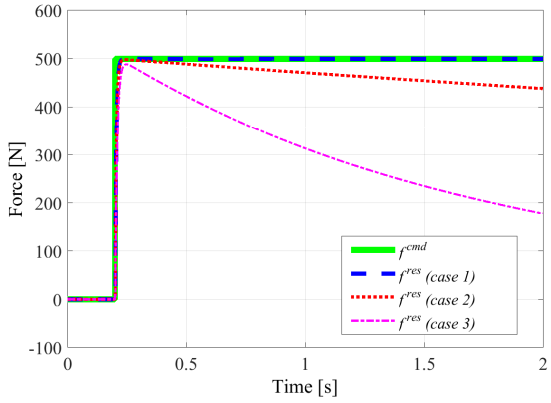

Fig. 5. Simulation with the conventional method for a 500 $[N]$ step force response f^{res}. The green solid line shows the force command f^{cmd}. The blue dashed, red dotted, and magenta chain lines show the force response in case 1, case 2, and case 3, respectively.

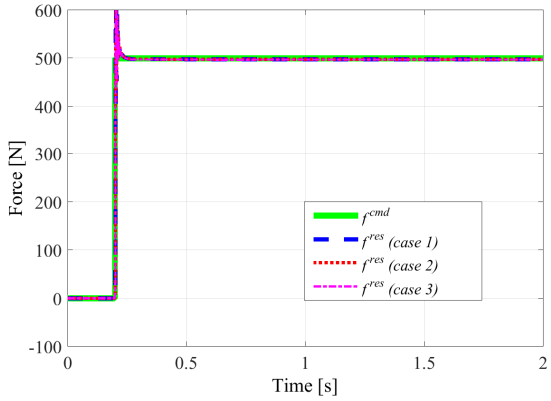

Fig. 6. Simulation with the proposed method for a 500 $[N]$ step response of the load force f^{res}. The green solid line shows the force command f^{cmd}. The blue dashed, red dotted, and magenta chain lines show the force response in case 1, case 2, and case 3, respectively.

actuation techniques, the bulk modulus β_e is usually treated as constant value. But actually, the bulk modulus can change according to the conditions such as oil temperature. Therefore, the modeling error of the bulk modulus can easily affect the performance. The proposed method is also supposed to solve the issue since the ideal bulk modulus is included in the black-box model, and the modeling error is compensated as disturbance.

B. Experiments

1) Experimental conditions: The experimental setup is shown in Fig. 7. The setup is consists of a hydraulic actuator, four pressure sensors, and a load cell. A spring was fixed to the load to generate a large amount of force. In the experiment,

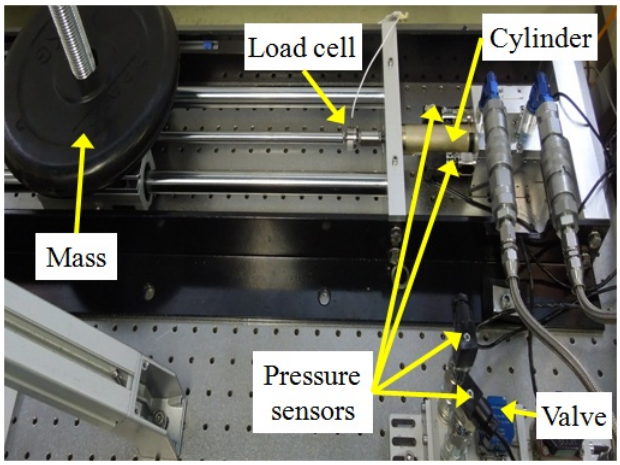

Fig. 7. Experimental setup.

TABLE III
NOMINAL PARAMETERS FOR THE $DOB1$ AND THE $DOB2$ IN EXPERIMENTS

$DOB1$	K_1	4.0	$[MPa/mA]$
	T_1	6.6×10^{-3}	$[s]$
$DOB2$	A_{pn}	2.0×10^{-4}	$[m^2]$
	M_n	3.0	$[kg]$

TABLE IV
CUTOFF FREQUENCIES IN EXPERIMENTS

Experimental case no.	$g_{V_1}[rad/s]$	$g_{V_2}[rad/s]$
case 1	0	0
case 2	100	0
case 3	200	0

the force command defined as (24) was applied to the setup.

$$f^{cmd} = \begin{cases} 1000/0.1 * time \ [N] \ (0 < time \leq 0.1) \\ 1000 \ [N] \ (0.1 < time) \end{cases} \quad (24)$$

The pressure responses p_s, p_t, p_a, p_b are measured by the pressure sensors and the load pressure response p_l was calculated. The force response f^{res} was measured by the load cell. As well as the simulation, the proportional gain K_p is used for the force controller. In the experiments, the proportional gain is set as $K_p = 0.002$. The other controller parameters used for the $DOB1$ and the $DOB2$ are shown in Table III. Here, the nominal parameters for the $DOB1$ are obtained by the modeling experiments in advance, and those for the $DOB2$ are obtained from the mechanical data sheet. The control software for this system was written in C/C++ language and it runs on a Linux kernel patched with real-time Xenomai. The sampling time was 1.0 $[ms]$. In this experiment, in order to demonstrate the effects of the proposed controller on the force control performance, the cutoff frequencies g_{V_1} and g_{V_2} are set as shown in Table IV. In order to evaluate the effects of the force control performance quantitatively, dynamic and static force control performance criteria are introduced. As the dynamic performance criteria, rise time and settling time are selected as follows:

- the rise time of the force response f^{res}:
  the time required for the response to rise from 10% to 90% of the final value.
- the settling time of the force response f^{res}:
  the time required for the response to reach and stay within $\pm 2\%$ of the final value.

For the evaluation of these criteria, a low pass filter with $20Hz$ cutoff frequency was used to avoid the effects of sensing noise in the load cell signal. Moreover, the static performance criteria are defined as follows:

- the maximum value of the force error $|f^{res} - f^{cmd}|$ in the steady-state data
- the average force error $f^{res} - f^{cmd}$ in the steady-state data
- the standard deviations of the force error $f^{res} - f^{cmd}$ in the steady-state data

Here, the data in last three seconds are used as the steady-state data.

2) Experimental results: Fig. 8 shows the result of the force step response by changing the cutoff frequencies of the $DOB1$ and the $DOB2$. As shown in Fig. 8 (b), in the transient state, the force response f^{res} rose faster when the cut off frequencies were higher. This is because the effect of the natural feedback which deteriorates the force responsiveness was compensated. Also, as shown in Fig. 8 (c), in the steady state, the steady state error became smaller when the cutoff frequencies were higher.

In addition, Table V and Table VI show the evaluation results of the dynamic and the static criteria, respectively. From Table V, with regard to the responsiveness, both the rise time and the settling time became shorter by increasing the cutoff frequencies. Also, from Table VI, with regard to the static accuracy, all results of the static criteria were improved by increasing the cutoff frequencies. From these results, it can be said that the responsiveness and accuracy are improved by the proposed method.

In this paper, the cutoff frequency of the $DOB2$ was set as 0 $[rad/s]$ since the same amount of the mass and the same cylinder were used in the experiments. In future, the improvement of the robustness against the load variations also should be shown by changing the cutoff frequency of the $DOB2$.

V. CONCLUSION

In this paper, the design method of a robust controller was proposed. The proposed controller takes the non-linearity of the hydraulic system into account, and compensates all the disturbance to the linearized hydraulic system and the mechanical system. The proposed controller consists of two types of disturbance observers. One compensates the disturbance to the linearized hydraulic dynamics, and the other compensates that to the load dynamics.

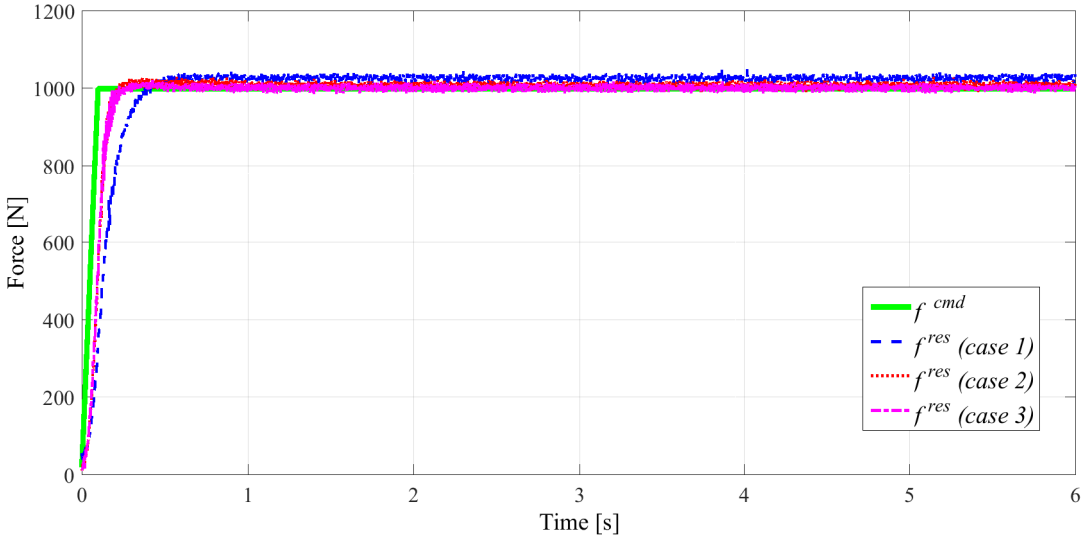

(a) Force command f^{cmd} and force response f^{res}

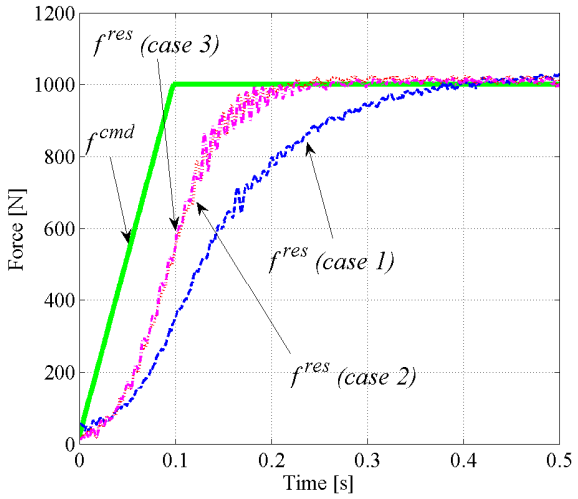

(b) The enlarged perspective view showing the transient state

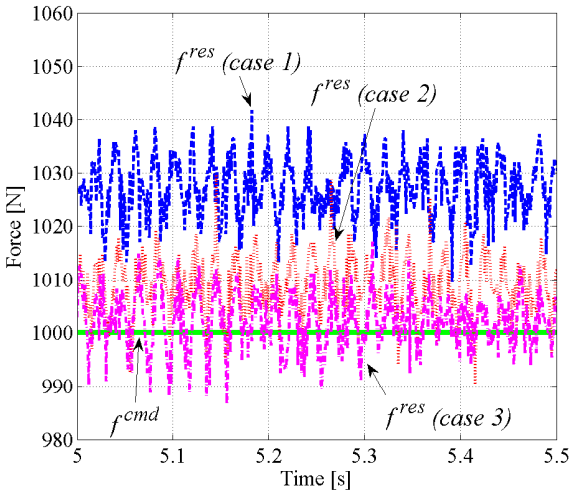

(c) The enlarged perspective view showing the steady-state

Fig. 8. Experimental results showing the force tracking by changing the cutoff frequencies of the $DOB1$ and the $DOB2$. The green solid line shows the force command f^{cmd}. The blue dashed, red dotted, and magenta chain lines show the force response in case 1, case 2, and case 3, respectively.

In simulation, the effect of the proposed method to improve the robustness against the modeling error was illustrated. In addition, the contribution of the proposed method for the hydraulic force control performance was confirmed through the experiments on a single cylinder test bench.

REFERENCES

[1] S. J. Dyke, B. F. Spencer Jr., P. Quast, and M. K. Sain, "Role of control-structure interaction in protective system design", *Journal of Engineering Mechanics ASCE*, vol. 121, pp. 322–338, Feb., 1995.

[2] A. Alleyne, R. Liu, and H. Wright, "On the limitations of force tracking control for hydraulic active suspensions", *In Proc. of American Control Conference*, pp. 43–47, June, 1998.

[3] A. Alleyne and R. Liu, "Systematic control of a class of nonlinear systems with application to electrohydraulic cylinder pressure control", *IEEE Trans. on Control Syst. Technol.*, vol. 8, no. 4, pp. 623–34, Jul., 2000.

[4] S. Sakai, and S. Stramigioli, "Passivity based control of hydraulic robot arms using natural Casimir functions: Theory and experiments", *In Proc. of IEEE/RSJ International Conference on Intelligent Robots and Systems*, pp. 538–544, Sept., 2008.

[5] Y. Lin, Y. Shi, and R. Burton, "Modeling and robust discrete-time sliding-mode control design for a fluid power electro-hydraulic actuator (EHA) system", *IEEE/ASME Trans. Mechatronics*, vol. 18, no. 1, pp. 1–10, Feb. 2013.

[6] J. Yao, Z. Jiao, and D. Ma, "Extended–state–observer–based output feedback nonlinear robust control of hydraulic systems with back–stepping", *IEEE Trans. on Ind. Electron*, pp. 6285–6293, vol. 61, No. 11, Nov., 2014.

[7] T. Boaventura, M. Focchi, M. Frigerio, J. Buchli, C. Semini, G. Medrano-Cerda, and D. Caldwell, "On the role of load motion compensation in high-performance force control", *In Proc. of IEEE/RSJ International Conference on Intelligent Robots and Systems*, pp. 4066–4071, Oct. 2012.

[8] M. Focchi, G. A. Medrano–Cerda, T. Boaventura, M. Frigerio, C. Semini, J. Buchli, and D. G. Caldwell, "Control of a hydraulically-actuated

TABLE V
EVALUATION RESULTS OF THE DYNAMIC CRITERIA

	rise time $[s]$	settling time $[s]$
$case\ 1$	0.22	0.44
$case\ 2$	0.11	0.23
$case\ 3$	0.11	0.23

TABLE VI
EVALUATION RESULTS OF THE STATIC CRITERIA

	max. error $[N]$	average error $[N]$	variance $[N]$
$case\ 1$	40.95	27.09	5.92
$case\ 2$	21.58	8.92	1.92
$case\ 3$	13.39	4.43	1.65

quadruped robot leg", *In Proc. of the IEEE International Conference on Robotics and Automation*, pp. 4182–4186, May, 2010.

[9] C. Semini, V. Barasuol, T. Boaventura, M. Frigerio, M. Focchi, D. G. Caldwell, and J. Buchli, "Towards versatile legged robots through active impedance control", *Journal of The International Journal of Robotics Research*, pp. 1003–1020, vol. 34, no. 7, June, 2015.

[10] T Boaventura, J. Buchli, C. Semini, and D. G. Caldwell "Model–based hydraulic impedance control for dynamic robots", *IEEE Trans. Robotics*, No. 99, pp. 1–13, Nov., 2015.

[11] Y. Cheng, "Robustness analysis and control system design for a hydraulic servo system", *IEEE Trans. Control Systems Technology*, vol. 2, no. 3, pp. 183–197, Sep., 2002.

[12] K. Ohnishi, M. Shibata, and T. Murakami, "Motion control for advanced mechatronics", *IEEE Trans. Mechatron.*, vol. 1, No. 1, pp. 56–67, Mar., 1996.